



ISSN: 2319-5967

ISO 9001:2008 Certified

International Journal of Engineering Science and Innovative Technology (IJESIT)

Volume 2, Issue 1, January 2013

Speed Estimation Of 3-Phase BLDC Motor Using Genetic Algorithm

Pawin Jawayon, Jiraphon Srisertpol

School of Mechanical Engineering, Suranaree University of Technology, Nakhon Ratchasima,
Thailand, 30000

Abstract— This paper describes a signal-based speed estimation of 3-Phase Brushless Direct Current (BLDC) motor using the relationship between commutation signal and Back Electromotive Force (Back-EMF). Both signals can directly be measured from each phase of motor's terminal. The relationship function between both signals is approximated and filtered to find Haft of Phase Voltage-Crossing Point. Genetic Algorithm (GA) is applied to estimate coefficients of the polynomial equation of relation between the variables σ , δ , β and commutation signal's period. The results of estimated speed are accurate more than 97 % and the average of overhead time is less than 9.0 ms.

Index Terms— 3-Phase BLDC Motor, Speed Estimation, Genetic Algorithm.

I. INTRODUCTION

The Brushless Direct Current (BLDC) motor has been used increasingly in both industrial and household applications [1]-[12] such as CD player, hard disk drives, medical tools, air conditioners etc. This is because the BLDC motor has better efficiency, good reliability, low maintenance, and power density. Presently, detection of speed and position of BLDC has two approaches. Firstly, the rotor's commutation signal is obtained by using the Hall-effect sensor. Secondly, by using the zero-crossing detection circuit, the rotor commutation signal of each phase can be estimated [3]-[7]. Mostly, the zero-crossing detection circuit uses op-amp to compare phase Back-EMF voltage with half of supply voltage. Therefore, there are many software-based methods proposed to find the zero-crossing of Back-EMF voltage for reducing the addition circuit. An artificial neural network (ANN) and a model reference adaptive system are used for finding a zero-crossing of Back-EMF in which the performance of the estimation is based on the properties of the motor [12]. The relation between the size of back-EMF voltage and the motor speed are applied to control the speed of motor using fuzzy logic in high speed range (more than 10,000 rpm) [13]. The artificial neural network is deployed to estimate the Back-EMF from voltage and current of each phase in low speed range [9]. Power rate reaching law sliding mode technique is applied to speed control for the inner-loop current control of BLDC motor and rejected load disturbance [14]. This paper presents the relationship of Back-EMF voltage, which is included within each phase voltage of motor. Phase voltage can be measured directly from each terminal of the motor. The function to estimate commutation signal from phase voltage is then created by using artificial intelligence techniques to find relations between each speed and commutation signal's function. The resulting commutation signal's frequency is then used as a frequency cut-off of low-pass filter for estimating Back-EMF signal from phase voltage. The filtered phase voltage signal or Back-EMF estimation can increase accuracy for estimating speed. The testing speed ranges in this work are approximately from 2,000 to 7,000 rpm. In this study we demonstrated a mathematical modeling of the BLDC motor and its electrical drives are described in Section II. Section III presents speed estimation procedure for the BLDC motor. Section IV and V are experimental results and conclusions.

II. PRINCIPLE OF BLDC MOTOR

A three-phase brushless DC motor has three induction coils with equivalent circuit of BLDC motors as described in the following section.

A. Mathematical Model of the BLDC Motor

The equivalent circuit of BLDC motor is shown in Fig.1. The dynamic equations of BLDC motor may be expressed in matrix form:

$$\begin{bmatrix} V_a \\ V_b \\ V_c \end{bmatrix} = R \begin{bmatrix} 1 & 0 & 0 \\ 0 & 1 & 0 \\ 0 & 0 & 1 \end{bmatrix} \begin{bmatrix} I_a \\ I_b \\ I_c \end{bmatrix} + \begin{bmatrix} L-M & 0 & 0 \\ 0 & L-M & 0 \\ 0 & 0 & L-M \end{bmatrix} \frac{d}{dt} \begin{bmatrix} I_a \\ I_b \\ I_c \end{bmatrix} + \begin{bmatrix} E_a \\ E_b \\ E_c \end{bmatrix} \quad (1)$$

The electromagnetic torque developed by the motor is given by

$$T_e = \frac{E_a I_a + E_b I_b + E_c I_c}{\omega} \quad (2)$$

The moment of inertia includes all inertia connected to the motor shaft, and damping constant includes the air friction and the bearing friction. Therefore, the torque equation is

$$J \frac{d\omega}{dt} + B\omega = T_e - T_l \quad (3)$$

- Where
- V_a, V_b, V_c are phase voltage [V],
 - I_a, I_b, I_c are phase current [A],
 - E_a, E_b, E_c are phase back EMF [V],
 - R is phase resistance [Ω],
 - L is self-inductance [H],
 - M is mutual inductance [H],
 - T_e is electromagnetic torque [N.m],
 - T_l is load torque [N.m],
 - ω is angular velocity [rad/s],
 - B is damping constant, [N.s/m]
 - J is moment of inertia [kg.m²].

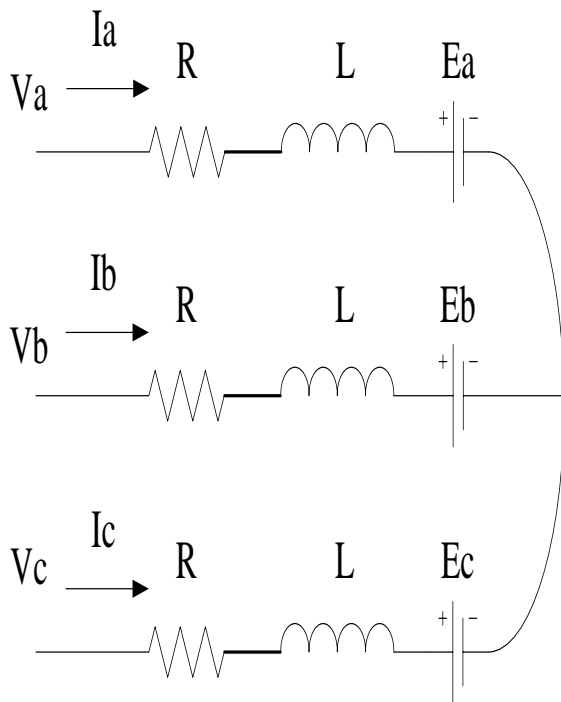


Fig.1 The Equivalent Circuit Of BLDC Motor

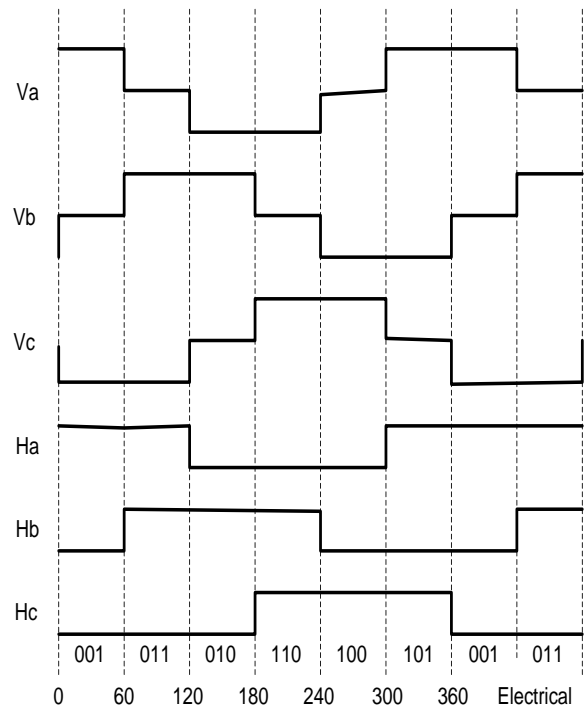


Fig.2 Six Step Commutation Sequence

B. The BLDC Motor Control

BLDC motors are driven by a three-phase inverter with six-step commutation sequence. The inverter is commutated every 60 degree electrical when Ha, Hb and Hc are Hall effect sensor signal of each phase as shown in Fig.2.

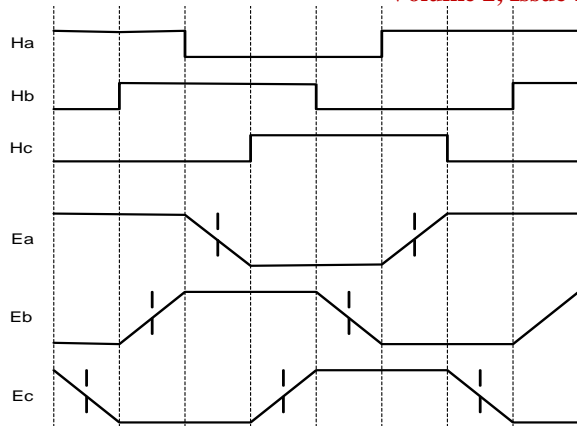


Fig.3 Back EMF signal and Hall Effect sensor

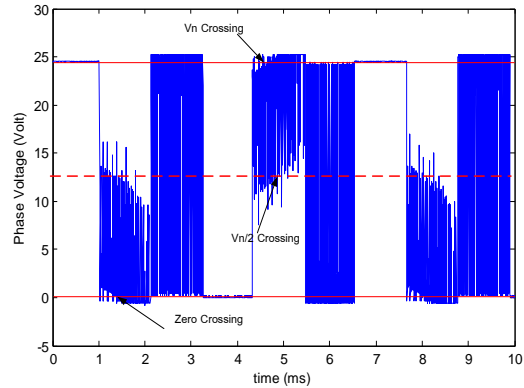


Fig.4 The zero $V_n/2$ and V_n crossing of each phase

C. BLDC Motor's Back EMF

The 2 coils are induced to rotate through a magnetic field; the induced voltage is created in this coils, call that “Back Electromotive force” or “Back-EMF”. The relation between Back-EMF signal and Hall effect sensor of each phase is shown in Fig. 3.

III. SPEED ESTIMATION PROCEDURE

The phase angle of half point of Back-EMF voltage of each phase lags from Hall effect sensors signal is 30 degrees. The half point of this Back-EMF voltage can be estimated by half of phase voltage of motor [4] as shown in Fig.4. The speed estimation procedure for the BLDC motor is described in next head respectively and speed estimation scheme is shown in Fig.5.

A. Define Band and Select Signal Range

The half point of Back-EMF crossing includes the half point of phase signal voltage ($V_n/2$) in which a band of interesting signal must be defined as in equation (4) before estimating the speed.

$$V_i^{(1)} = \begin{cases} \frac{V_n}{2}, & \frac{V_n}{2} - \frac{\delta}{2} \leq V_i \leq \frac{V_n}{2} + \frac{\delta}{2} \\ 0, & \text{otherwise} \end{cases} \quad (4)$$

Where δ is window size of interesting band, V_i is phase voltage at I and V_n is supply voltage.

The selected signal is demonstrated in Fig. 6. The signals that pass the selected band depend on the window size of interesting band (δ).

B. Find the Selected Signal's Edge

Once the selected signal is defined, the envelope of the selected signal can be found by Moving Average (MA) as shown in equation (5). The envelope of the selected signal in Fig.7 shows the highest density area of the half point of phase voltage crossing.

$$V_i^{(2)} = \frac{\sum_{j=i-\sigma}^{i-1} V_j^{(1)}}{\sigma} \quad (5)$$

Where $V_j^{(1)}$ is selected signal at j ,
 $V_i^{(2)}$ is MA filtered signal at i ,
 σ is window size of MA

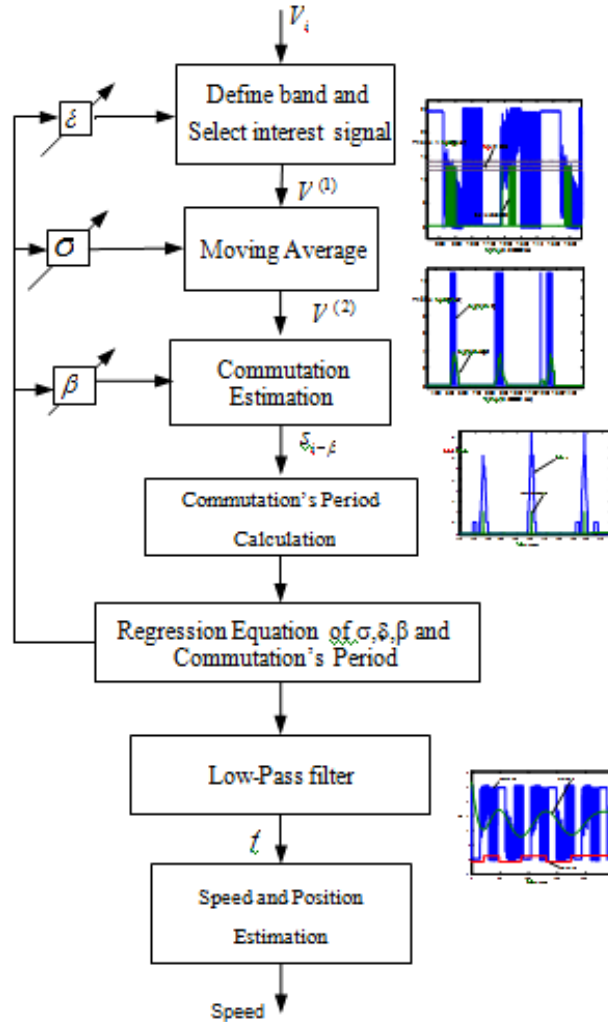


Fig.5 Speed Estimation Scheme

C. Find the Selected Signal's Edge

The selected signal which is filtered by the MA function shows the highest density area of the half point of phase voltage crossing. The local maximum in this area can be estimated by (6) and (7). The result is shown in Fig. 8.

$$L_{\max_i} = \begin{cases} V_i^{(2)} & , V_i^{(2)} > L_{\max_{i-1}} \\ L_{\max_i} & , \text{otherwise} \end{cases} \quad (6)$$

$$s_{i-\beta} = \begin{cases} 1 & , L_{\max} \in [V_{i-\beta}^{(2)}, V_i^{(2)}] \\ 0 & , \text{otherwise} \end{cases} \quad (7)$$

where $L_{\max,i}$ is local maximum
 $s_{i-\beta}$ is estimated commutation signal at $i-\beta$
 $V_i^{(2)}$ is filtered signal at i
 β is previous time range from i

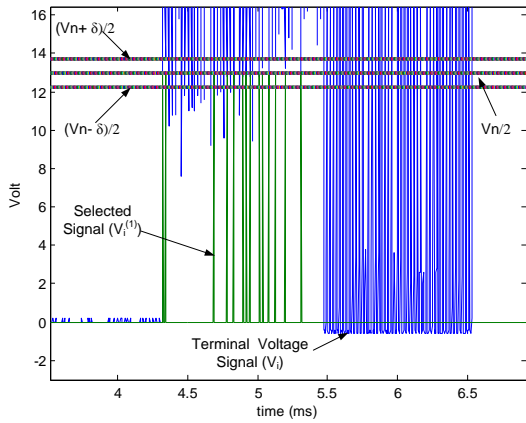


Fig.6 Back EMF signal and Hall effect sensor

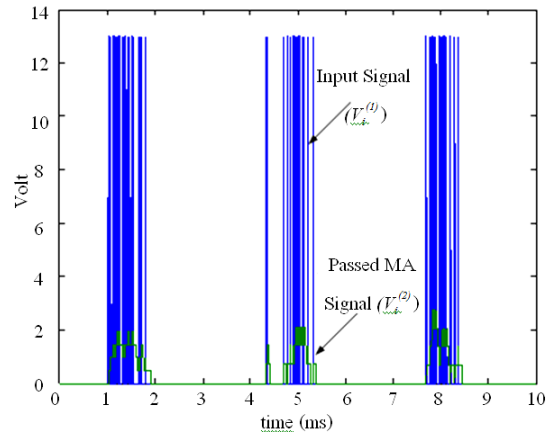


Fig.7 The zero $V_n/2$ and V_n crossing of each phase

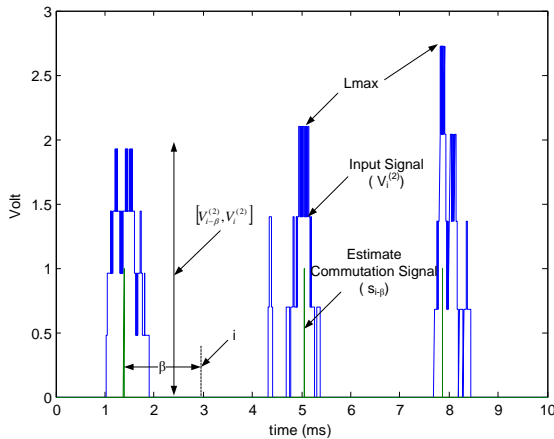


Fig.8 The MA filtered signal ($V_i^{(2)}$) and estimated Commutation signal ($S_{i-\beta}$)

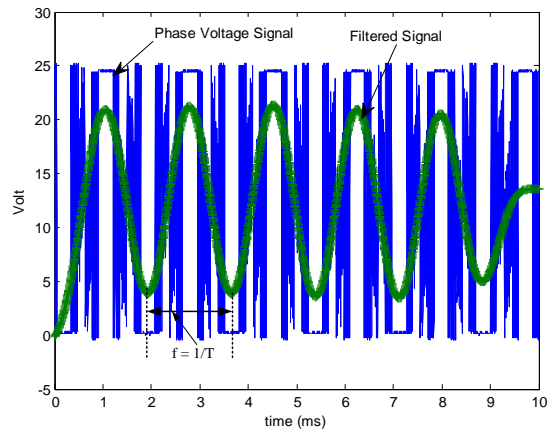


Fig.9 Phase voltage signal and filtered signal

D. Estimate Back-EMF by Low-Pass Filter

The phase voltage signal is included in the Back-EMS signal. Both signals can be separated by using low-pass filter with frequency cut-off derived from the above method. This work uses Butterworth low-pass filter to separate Back-EMF from phase voltage signal as shown in Fig. 9.

E. Speed Calculation

The rotor speed can be calculated from frequency of estimated commutation of each phase using equation (8).

$$n = \frac{f \times 120}{Z_{Pol}} \tag{8}$$

where n is motor shaft speed [rpm],
 f is frequency of commutation signal [Hz],
 Z_{Pol} is number of motor's magnetic poles

Table I Error of the Fitness Curve from GA

Population	$e_{\sigma}, \%$	$e_{\delta}, \%$	$e_{\beta}, \%$
20	198.4	63.60	133.97
100	3.37	75.36	18.03



ISSN: 2319-5967

ISO 9001:2008 Certified

International Journal of Engineering Science and Innovative Technology (IJESIT)

Volume 2, Issue 1, January 2013

250	15.93	9.98	7.62
500	6.54	3.03	8.59
1,000	6.59	8.29	7.11

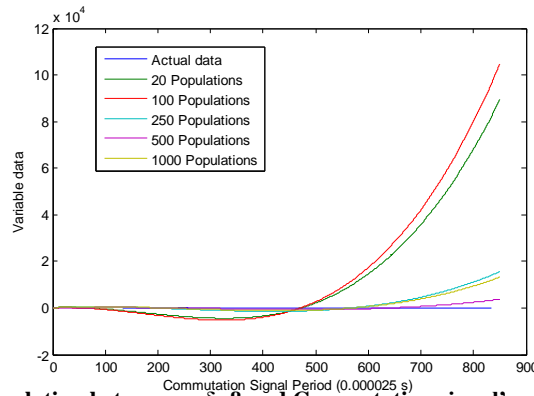


Fig.10 Fitness curve of relation between σ , δ , β and Commutation signal's period with population size of GA

Table II Relationship between σ , δ , β and Commutation Signal's Period

Commutation signal's period (x 0.00025 ms)	σ	δ	β	Speed (rpm)	Cutoff frequency (Hz)
391	12	50	70	2,386	500
368	12	50	60	2,523	550
324	12	45	50	2,874	550
303	10	45	40	3,121	600
282	10	45	40	3,294	600
268	10	30	15	3,464	650
222	10	30	15	4,169	700
218	10	30	15	4,249	750
215	10	30	15	4,333	750
201	10	30	15	4,600	750
193	10	30	15	4,836	850
185	10	30	15	4,975	900
181	10	30	15	5,145	900
169	8	30	15	5,486	1,000
152	8	25	10	6,040	1,150
143	8	25	10	6,454	1,250

F. Relation between σ , δ , β and Commutation Signal's Period

In each commutation frequency or each speed, variables σ , δ and β in each step are different. Therefore, the relation between variables σ , δ , β for each speed must be calculated to be able to use in all speed range. The Genetic Algorithm (GA) [15] is applied to estimate coefficients of the polynomial equation of relation between the variables σ , δ , β and commutation signal's period. The root mean square error of each parameter (e_σ , e_δ , e_β) decreases when population size of each generation increases as shown in Table I and Fig.10. The fitness curve from GA is more accurate of relation between σ , δ , β and commutation signal's period. The calculation time, however, increases also. The relationship between σ , δ , β and cutoff frequency for each speed is shown in Table II. Relation between σ , δ , β and the previous commutation signal's period T_{i-1} is shown in equation (9)

$$\begin{bmatrix} \sigma \\ \delta \\ \beta \end{bmatrix} = \begin{bmatrix} 0 & -0.0192 & 5.0974 \\ 0.0002 & -0.0894 & 35.2124 \\ 0.0004 & 0.0802 & 58.6711 \end{bmatrix} \begin{bmatrix} T_{i-1}^2 \\ T_{i-1} \\ 1 \end{bmatrix} \quad (9)$$

IV. EXPERIMENTAL RESULTS

In experiment, the BLDC motor is MAXON EC 45 Flat motor 45 mm, brushless, 50 Watt with the data as shown in Table III. The motor control is MAXON 1-Q-EC Amplifier AECS 35/3. The experimental setup is used Manchester M7 9RH for speed measurement, Tektronix TDS 1001B 40 MHz for data display and signal conditioning by MATLAB. The speed estimation method is divided into two steps. The first step is to find the frequency of the commutation signal using the each function in section III. The resulting frequency can be used to estimate speed but the result has more error. Therefore, the commutation signal's frequency is known, the frequency cut-off of Butterworth low-pass filter can be applied to get the high accuracy for speed estimation.

Table III Motor Data

Symbol	Parameter	Data
V_v	Nominal voltage	24.0 V
-	No load speed	6800 rpm
I_{max}	Nominal current (max. continuous current)	2.58 A
R	Terminal resistance phase to phase	1.03 Ω
L	Terminal inductance phase to phase	0.450 mH
T_e	Torque constant	33.5 mNm / A
J	Rotor inertia	135 gcm ²
P	Pole permanent magnet	16

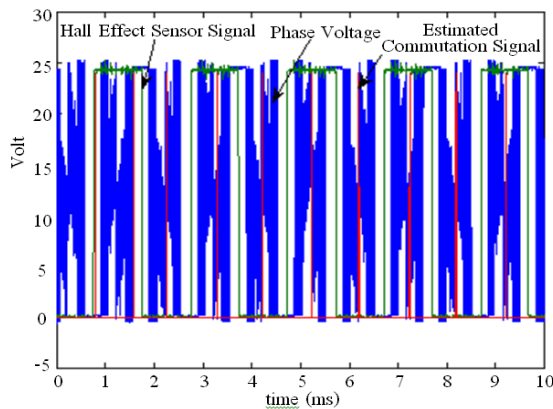


Fig.11 Output signal at speed 3,785 rpm

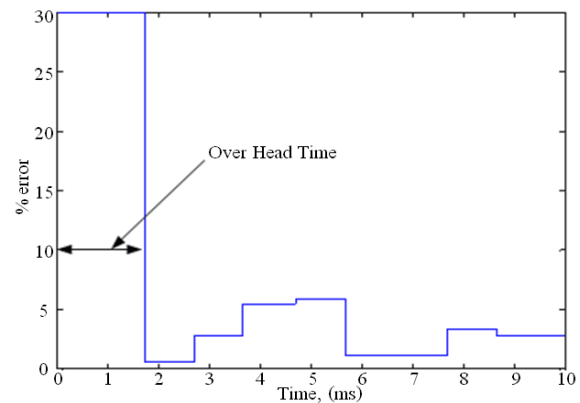


Fig.12 %error of estimated speed before filtering at speed 3,785 rpm

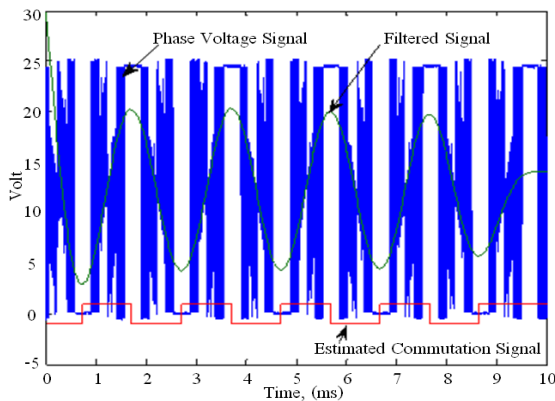


Fig.13 Phase voltage and filtered signal at speed 3,785 rpm

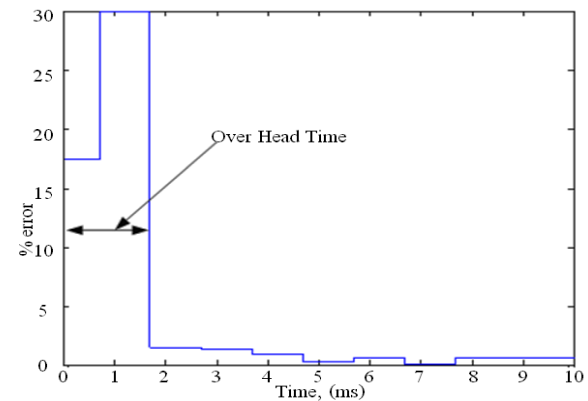


Fig.14 %error of estimated speed at speed 3,785 rpm

A. Low Speed Estimation

Low speed range, Hall effect sensor signal, phase voltage signals and estimated signals at speed 3,785 rpm in Fig. 11, shows that the signal is estimated to have periods near the period of Hall effect sensors signals. The parameters σ , δ and β at speed 3,785 rpm are 10, 30 and 15, respectively. The percentage error of estimated speed without using the low-pass filter shows in Fig 12. Once the frequency from previous step is used as the cutoff frequency of low pass filter, the frequency of the back-EMF can be estimated as shown in Fig. 13. The frequency of the back-EMF is used to estimate for speed again which is more accurate but overhead time of calculation increases. The percentage error of the estimated speed is shown in F

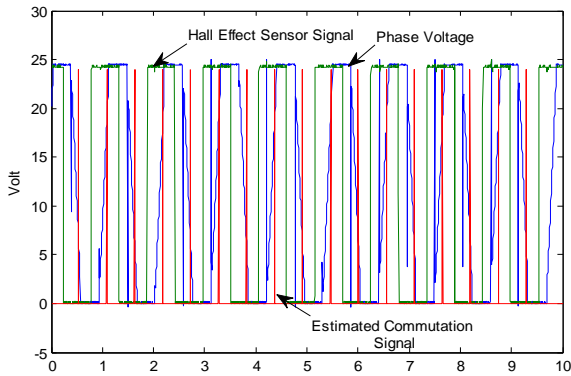


Fig.15 Output signal at speed 6,885 rpm

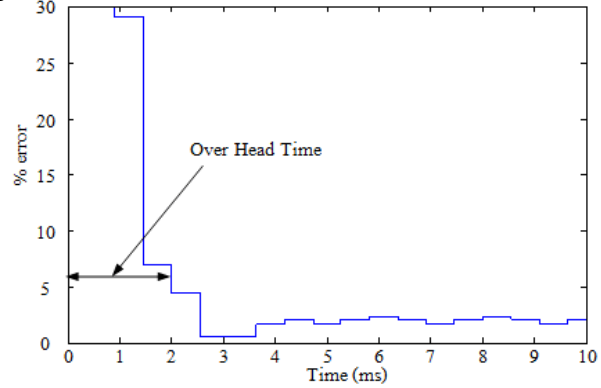


Fig.16 %error of estimated speed before filtering at speed 6,885 rpm

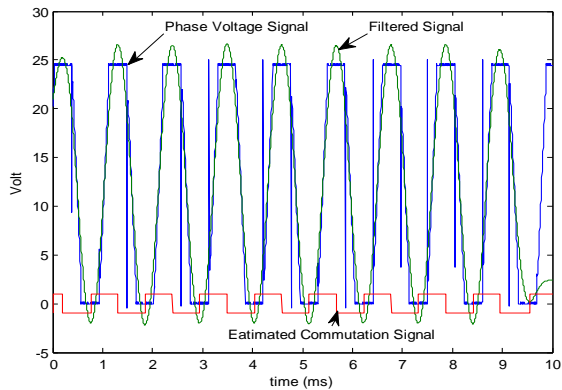


Fig.17 Phase voltage and filtered signal at speed 6,885 rpm

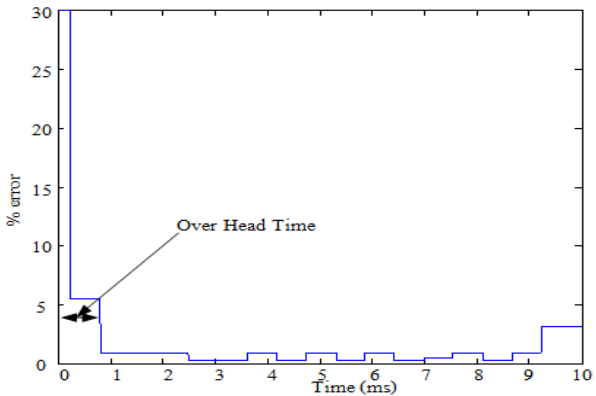


Fig.18 %error of estimated speed at speed 6,885 rpm

B. High Speed Estimation

High speed range, Hall effect sensor signal, phase voltage signals and estimation signals at speed 6,885 rpm in Fig. 15, show that the signal is estimated to have periods nearby the period of Hall effect sensors signals. The parameters σ , δ and β at speed 6,885 rpm are 8, 25 and 10, respectively. The percentage error of estimation speed without using the low-pass filter is shown in Fig 16. Once the frequency from previous step is used as the frequency cut-off of low pass filter, the frequency of the Back-EMF can be estimated as shown in Fig. 17. The approximate of frequency of the Back-EMF is used to estimate for speed again which is more accurate but overhead time of calculation increases. The percentage error of estimated speed is shown in Fig. 18. Fig.19 and Table IV shows the estimated speed in range of 2,000 to 7,000 rpm. At high range overhead time are decreased and the estimated speed error is less than the lower speed range. The damping force has effected in the low speed range more than high speed range. Thus, the relationship between σ , δ , β and commutation signal's period for low speed must be improved.



ISSN: 2319-5967

ISO 9001:2008 Certified

International Journal of Engineering Science and Innovative Technology (IJESIT)

Volume 2, Issue 1, January 2013

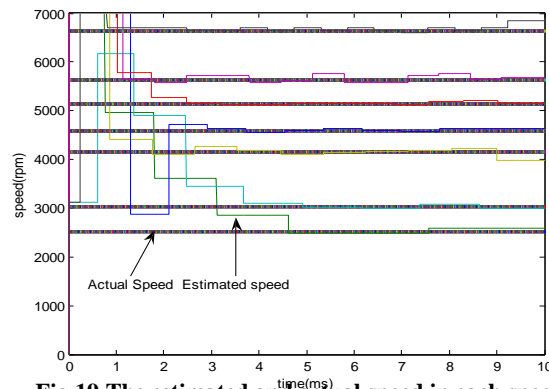


Fig.19 The estimated and actual speed in each speed

Table IV Error and Overhead Time in each Speed

Speed (rpm)	Overhead Time (ms)	Error (%)
2108	8.23	1.28
2523	7.62	2.11
3038	6.68	1.26
3605	4.81	1.3
3994	4.4	2.1
4600	4.2	0.87
5145	3.8	0.54
5649	3.14	1.01
6040	3.17	0.52
6637	0.79	0.78
6885	1.04	0.75

V.CONCLUSION

This paper demonstrates speed estimation of 3-phase BLDC motor using Genetic Algorithm. The relationship between commutation signal and Back-EMF can be estimated speed of BLDC motor. The performance of the proposed method is verified by the experimental results in a speed range of 2,000 to 7,000 rpm. The proposed method can reduce the cost of speed measuring and can use in speed control system. The overhead time is less than 9.0 ms and the average percentage error of estimated speed is less than 2.

ACKNOWLEDGMENT

The authors would like to thankfully acknowledge the research grant from Suranaree University of Technology.

REFERENCES

- [1] S.M.M. Mirtalaei, J.S.Moghani, K. Malekian and B. Abdi, "A Novel Sensor less Control Strategy for BLDC Motor Drives Using a Fuzzy Logic-based Neural Network Observer", in Proceeding of International Symposium on Power Electronics, Electrical Drives, Automation and Motion, Ischia, Italy, 2008, pp.1491-1496.
- [2] H. Lu, L. Zhang, and W. Qu, "A New Torque Control Method for Torque Ripple Minimization of BLDC Motors with Un-Ideal Back EMF", IEEE Transactions on Power Electronics, vol.23, no.2, pp.950-958, March.2008.
- [3] J. Shao, D. Nolan, and T. Hopkins, "Improved Direct Back EMF Detection for Sensor less Brushless DC (BLDC) Motor Drives", in Proceeding of IEEE APEC, Florida, USA, 2003, pp.300-305.



ISSN: 2319-5967

ISO 9001:2008 Certified

International Journal of Engineering Science and Innovative Technology (IJESIT)

Volume 2, Issue 1, January 2013

- [4] S.G. Lee, D.K. Kim, D.S. Shin, B.T. Kim, B.I. Kwon, and Y.C. Lim, "A Study on Low-Cost Sensor less Drive of Brushless DC Motor for Compressor Using Random PWM", in Proceeding of International Conference on Electrical Machines and Systems, Seoul, Korea, 2007, pp.920-925.
- [5] T.S. Kim, J.S. Ryu, and D.S. Hyun, "Sensor less Drive of Brushless DC Motors Using an Unknown Input Observer", in Proceeding of Annual Conference of the IEEE Industrial Electronics Society, North Carolina, USA, 2005, pp.1413-1418
- [6] A. Sathyan, M. Krishnamurthy, N. Milivojevic, and A. Emadi, "A Low-Cost Digital Control Scheme for Brushless DC Motor Drives in Domestic Applications", in Proceeding of International Electric Machines and Drives Conference, Miami, Florida, 2009, pp.76-82.
- [7] J. Shao, "An Improved Microcontroller-Based Sensor less Brushless DC (BLDC) Motor Drive for Automotive Applications", IEEE Transactions on Industry Applications, vol.42, no.5, pp.1216-1221, September/October.2006.
- [8] Y.W. Sheng, L. Hai, L. Hong, and Y. Wei, "Sensor less Direct Torque Controlled Drive of Brushless DC Motor based on Fuzzy Logic", in Proceeding of 4th IEEE Conference on Industrial Electronics and Applications, Xi'an, China, 2009, pp.3411-3416.
- [9] C.L. Xia, and W. Chen, "Sensorless Control of Brushless DC Motors at Low Speed using Neural Networks," in Proceeding of the International Conference on Machine Learning and Cybernetics, Guangzhou, China, 2005, pp.1099-1103.
- [10] T.H. Kim, B.K. Lee, and M. Ehsani, "Sensor less Control of the BLDC Motors from Near Zero to High Speed", IEEE Transactions on Power Electronics, vol.19, no.6, pp.306-312, November.2004.
- [11] S. Poonsawat, and T. Kulworawanichpong, "Speed Regulation of a Small BLDC Motor using Genetic-Based Proportional Control," International Journal of Intelligent Systems and Technologies, vol.3, no.4, pp.220-225, Autumn.2008.
- [12] M.E. Elbuluk, L. Tong, and I. Husain, "Neural-Network-Based Model Reference Adaptive Systems for High-Performance Motor Drives and Motion Controls", IEEE Transactions on Industry Applications, vol.38, no.3, pp.879-886, May/June. 2002.
- [13] J.S. Wen, C.H. Wang, Y.D. Chang, and C.C. Teng, "Intelligent Control of High-Speed Sensor less Brushless DC Motor for Intelligent Automobiles", in Proceeding of IEEE International Conference on Systems, Man and Cybernetics, San Antonio, TX USA, 2008, pp.3394-3398.
- [14] Jagat Jyoti Rath, "Effective Speed Control in 3-Phase BLDC Motor by Reaching Law based Sliding Mode Technique", International Journal of Computer Applications vol.43, no.16, pp.25-32, April 2012.
- [15] A. Srikeaw, "Computational Intelligence", 1st Edition, Suranaree University of Technology, 2009, pp.65-160.

AUTHOR BIOGRAPHY

Jawayon P. is graduate student in School of mechanical engineering, Institute of engineering, Suranaree University of Technology, Nakhon Ratchasima, Thailand. He got Bachelor degree in Computer Engineering from Prince of Songkla University in Thailand. His research interests are in area of the embedded system.

Srisertpol J. is an Assistant Professor in School of mechanical engineering, Institute of engineering, Suranaree University of Technology, Nakhon Ratchasima, Thailand. He got Ph.D degree in System Analysis, Control and Processing Information from St.Petersburg State University of Aerospace Instrumentation in Russia. He is head of system and control engineering laboratory. His research interests are in area of the mathematical modeling, adaptive system and vibration analysis.